CHAPTER IV
RESULT AND DISCUSSION

4.1 Preparation and Characterization of Chitosan

4.1.1 Chitosan Production

Shrimp shells consist of three major components which are chitin, calcium carbonate, and protein. Calcium carbonate and protein can be removed by solvent extraction and chitin will be obtained as the remaining substance. Whereas chitosan is the name given to the total, partially (majorly) deacetylate form chitin.

In this research, chitosan was prepared from shells of *Litopeneous vannamei* shrimp by demineralization with HCl, deproteinization with 4% NaOH and deacetylation with 50% NaOH in order to remove the calcium carbonate, protein, and the acetyl group of N-acetyl glucosamine repeating units in shrimp shells, respectively. Yield of chitin and chitosan production from shrimp shell are shown in Table 4.1

Table 4.1 Yield of chitin and chitosan production from shrimp shell

Materials	Yield*(%)
Shrimp shell	100
Product after demineralization	55.55
Product after deproteinization (chitin)	36.25
Product after deacetylation (1st alkali treatment)	28.57
Product after deacetylation (2nd alkali treatment)	25.44
Product after deacetylation (3rd alkali treatment)	21.44
Product after deacetylation (4th alkali treatment)	19.82

* dry weight basis

4.1.2 Determination of the Degree of Deacetylation (%DD) of Chitosan

The characteristic of chitosan that may be varied as required for a particular application are the degree of deacetylation (compared to chitin) and the molecular weight (Rabea *et al*, 2003). The method used to determine degree of deacetylation of chitin and chitosan were based on infrared spectroscopic measurement by Sannan *et al.* (1978) and Baxter *et al.* (1992), respectively. The degree of deacetylation (DD) was calculated from equation 4.1 and 4.2 respectively.

$$DD = 98.03\text{-}34.68\ (A_{1550}/\ A_{2878}) \tag{4.1}$$

$$DD = 100\text{-}\ [(A_{1655}/A_{3450}) \times 115] \tag{4.2}$$

where   DD = degree of deacetylation , A_{1550} = absorbance at 1550 cm^{-1},

A_{2878} = absorbance at 2878 cm^{-1}, A_{1655} = absorbance at 1655 cm^{-1},

A_{3450} = absorbance at 3450 cm^{-1}

Chitosan has more extent of amino groups than acetamide groups at C2 position of N-acetyl glucosamine repeating units. The degree of deacetylation of chitosan depends on the nature of chitosan resources and the conditions used during deproteinization. The chitosan used in this study was inevitably subjected to N-deacetylation process under alkaline condition and heating. The result in figure 4.1 shows that the degree of deacetylation (%DD) of chitosan increased with increasing the number of alkali treatment cycles, but the degree of deacetylation (%DD) of chitosan became constant after alkali treatment of chitosan for three times. According to the method of Baxter *et al.* (1992), the degree of deacetylation of chitin calculated from FTIR spectrum in figure 4.2 was 8% and those of chitosan were 83% and 95% for first and second treatment cycles, respectively, and 97% for both third and forth treatment cycles.
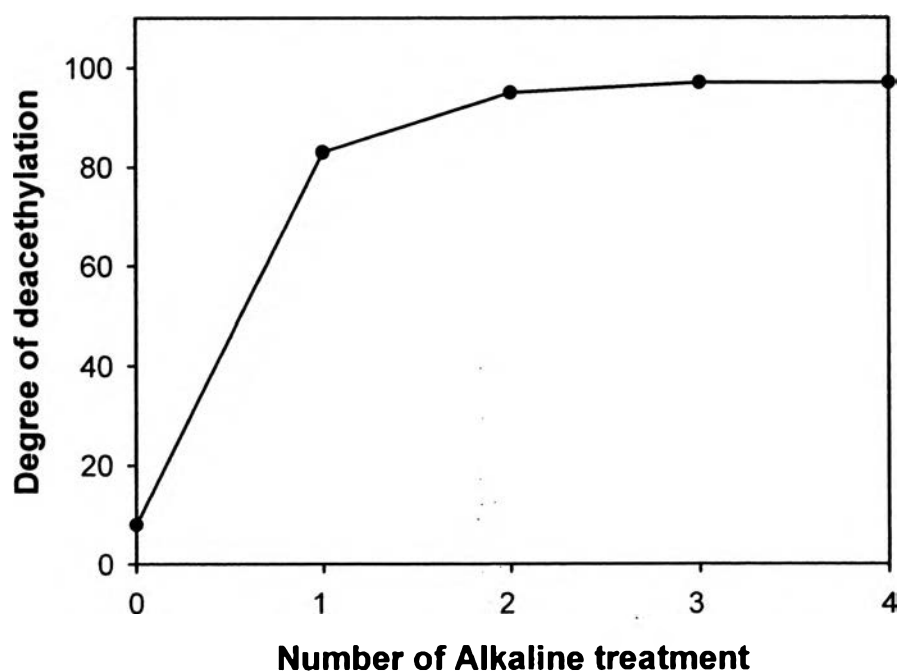
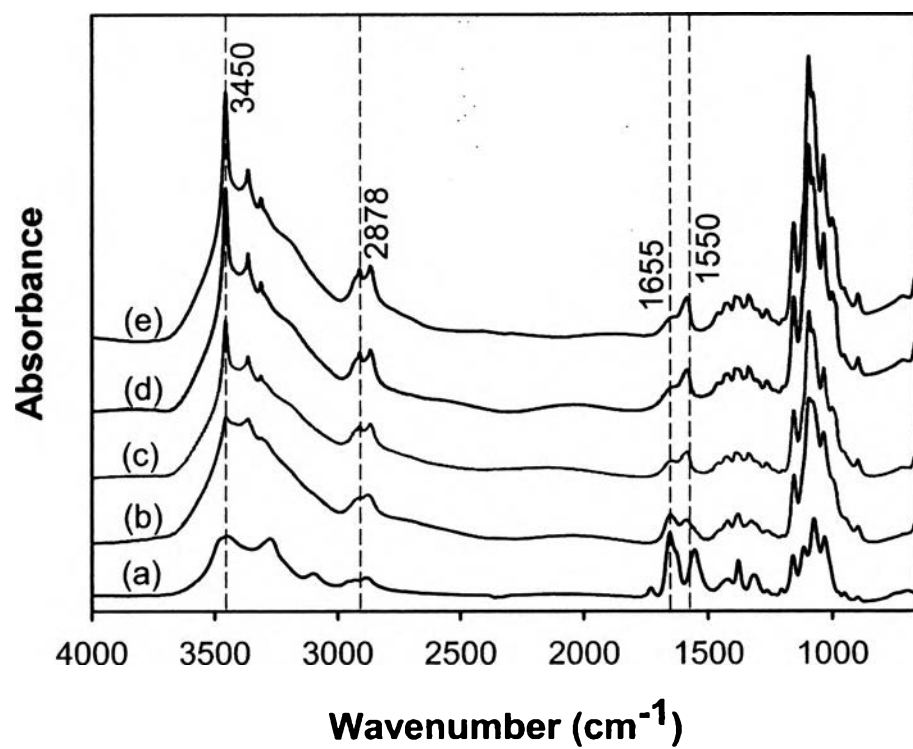**Figure 4.1** Effect of number of alkaline treatment on the degree of deacetylation of chitosan.

Figure 4.2 FTIR spectra of chitin and chitosan: (a) chitin, (b) 1st deacetylation, (c) 2nd deacetylation, (d) 3rd deacetylation, (e) 4th deacetylation.

4.1.3 Determination of the Molecular Weight of Chitosan

The molecular weight of chitosan was resolved based on viscosity measurement by the method of Wang *et al.* (1991). The intrinsic viscosity was determined from the extrapolation of the plot between $[\eta_{sp}]/c$ versus chitosan concentration (g/dl) and ln $[\eta_{rel}]/c$ versus chitosan concentration (g/dl). The viscosity-average molecular weight of chitosan was then calculated using the Mark-Houwing equation (equation 4.3)

$$[\eta] = 6.59 \times 10^{-5} M_v^{0.88} \qquad (4.3)$$

where $[\eta]$ = Intrinsic viscosity (dl/g)

M_v = Viscosity-average molecular weight

K and a are the coefficients related to the Ubbelohde tube and the molecular weight of sample

**Table 4.2** Characteristics of chitosan treated samples

Number of alkali treatment	Degree of deacetylation (%DD)	Molecular weight (kDa)
1	83	1100
2	95	968
3	97	807
4	97	704

When the number of alkali treatment increased, the degree of deacetylation of chitosan increased whereas molecular weight of chitosan decreased. The chitosan used in this study was the 3rd alkali treatment because it has high degree of deacetylation and high molecular weight.

4.2 Characterization of modified surfaces

4.2.1 Effect of Plasma Treatment Time on Contact Angle

Knowing that radicals usually react with dioxygen of air, the optimal parameters for plasma treatment (incident power and time of treatment) were deduced from the minimum value of the water contact angle (Marais *et al.*, 2005). Figure 4.3 shows the variation curve of water contact angle versus DBD plasma treatment time of four polymeric films. The water contact angle dramatically decreases with the increase of treatment time of about 5 s. It continuous to decrease with the prolonged treatment time but the contact angle was hardly decreased after plasma treatment time beyond 10 s or more. After plasma treatment time for 10s, the water contact angle values of PVC films decreased from $71.5°$ to $46.4°$, that of PE films decreased from $95.2°$ to $45.7°$, that of PP films decreased from $94.8°$ to $50.3°$, and that of PLA films decreased from $72.4°$ to $53.8°$. The decreasing of water contact angle suggests that the DBD plasma treatment increased the hydrophilicity of the plasma-treated polymeric film surfaces. The plasma treatment introduces polar groups, such as peroxides and other oxygenated species, onto the C–C bonds. The polar groups, in turn, give rise to a more wettable surface, as indicated by the contact angle data (Ding *et al*, 2004).
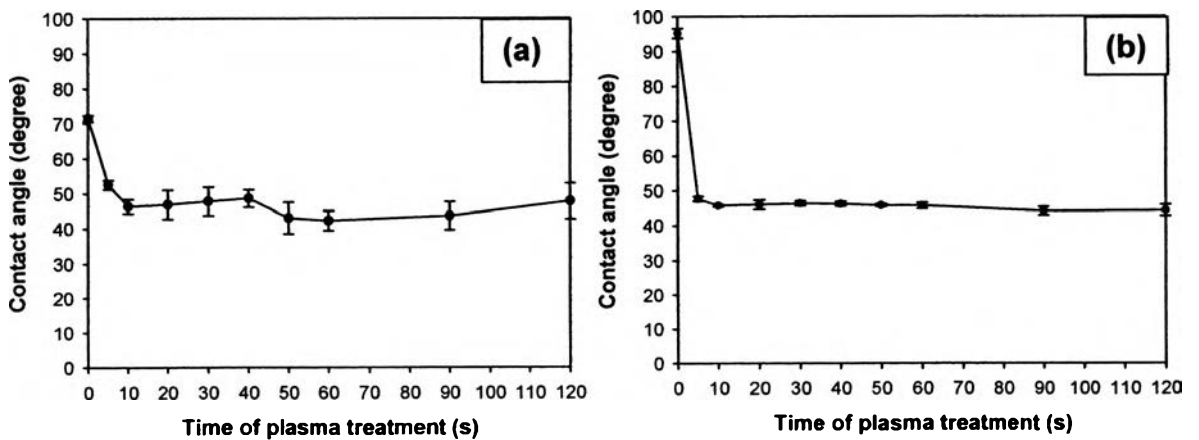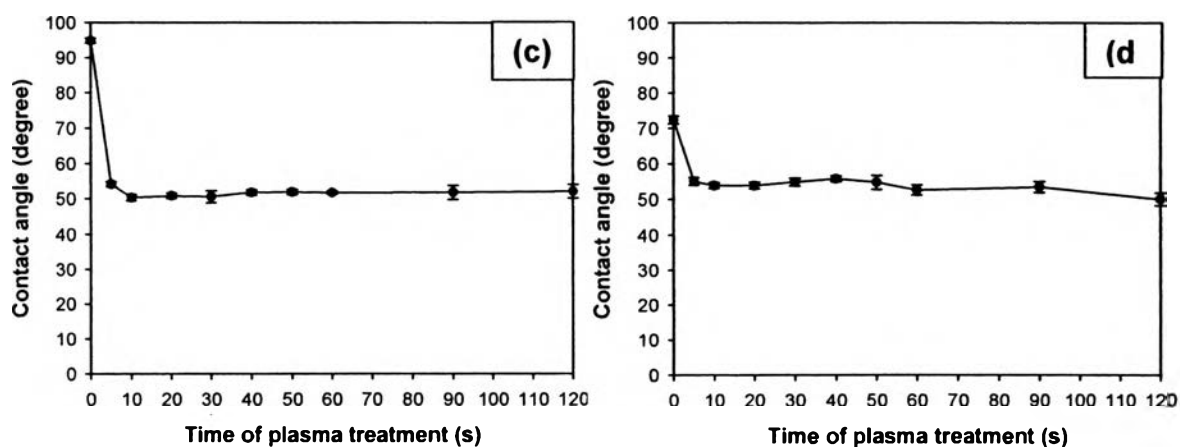
Figure 4.3 Variation curve of water contact angle versus DBD plasma treatment time of four polymeric films; (a) PVC films, (b) PE films, (c) PP films, and (d) PLA films.

4.2.2 Effect of Plasma Treatment Time on The Mechanical Properties

The mechanical properties after prolonged treatment time of all polymeric films were determined. The results for tensile strength and elongation at break for all the plasma-treated films with different plasma treatment time are shown in Figure 4.4 and 4.5, respectively. In the case of PVC films, both tensile strength and elongation at break slightly decreased with prolonged plasma treatment time. For increasing treatment time (30 s), a significant decrease (p<0.05) is obviously observed of the tensile strength from 7.67 ± 0.83 to 3.05 ± 0.21 compared between the untreated and the plasma treated films for 30 s. This result may be explained that the prolonged treatment time made the loss of additives and plasticizers from the flexible PVC films leading to decrease of the mechanical properties. In the case of PE films, both tensile strength and elongation at break slightly decreased after plasma treatment time for 5 s and become no statically significant difference in mechanical properties when prolonged treatment time. In the case of plasma-treated PP and PLA films, no statistically significant differences are observed in mechanical properties of all plasma treatment time. On the other hand, a little difference was observed on plasma-treated PVC and PE films either tensile strength or elongation at break before and after plasma treatment for 30s. This reduction of tensile strength and elongation at break in agreement with the work of Shin *et al.*, (2002) and Gancarz *et al.*, (1999), who reported that the decrease of tensile strength and

elongation at break can be attributed to the scission of the molecular chains on the surface. This is a negative result due to the surface etching phenomenon occurred during plasma treatment. Only for PP and PLA films exhibit very similar mechanical properties and variation are quite small after treatment time for 30 s. This suggests that the surface etching phenomenon does not affect the mechanical properties of PP and PLA films.
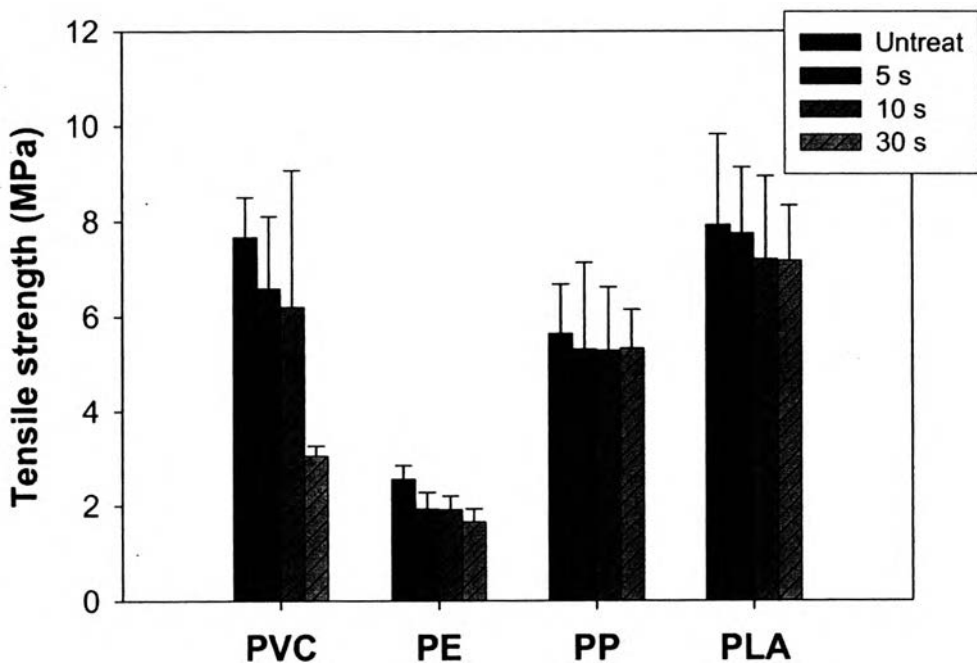

Figure 4.4 The influence of plasma treatment time on the tensile strength of four polymeric films.
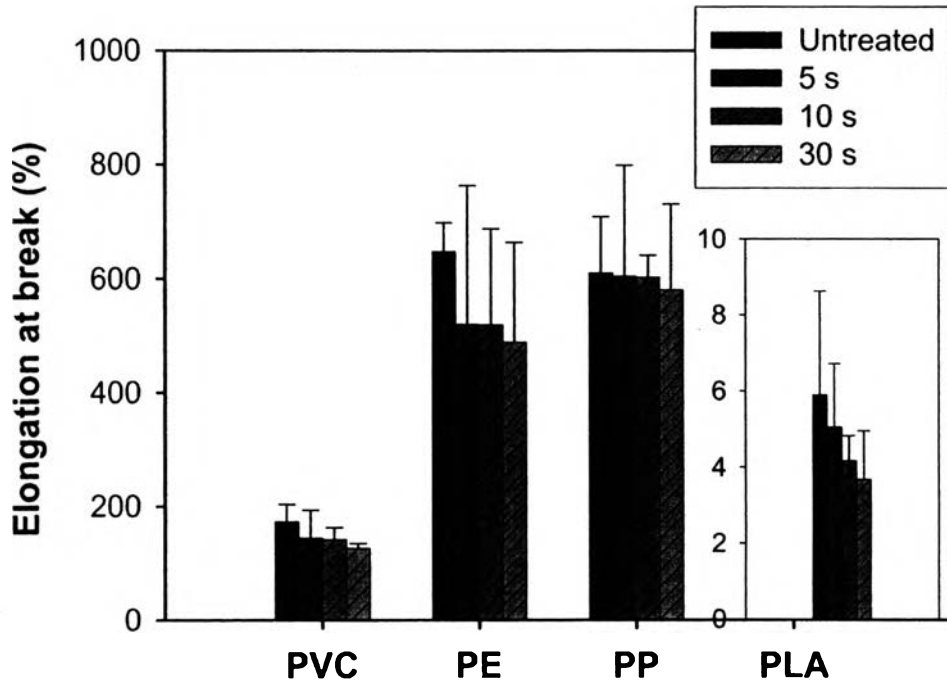
Figure 4.5 The influence of plasma treatment time on percent elongation at break of four polymeric films.

4.2.3 Chemical Composition of DBD Plasma Treated Polymeric Surface

Surface chemical modifications induced by DBD plasma treatment in air atmospheric are characterized by X-ray photoelectron spectroscopy. The XPS determines both qualitative and quantitative of chemical compositions in the polymeric surface. The XPS spectra of PVC, PE, PP and PLA films before and after DBD plasma treatment are shown in Figure 4.6, 4.7, 4.8 and 4.9, respectively.

The XPS spectra of before and after plasma treatment on polymeric surfaces can be divided into three components: a component at 285.0 eV assigned to C–C/C–H bond, a component at 286.7 eV assigned to C–O bond and a component at 289.0 eV assigned to O–C=O bond (Briggs and Seah, 1990). After plasma treatment of all polymeric films, the hydrophilic chemical compositions of oxygen content were increased but the hydrophobic compositions of the atomic concentration of carbon are decreased. Only the surface of PVC films treated by DBD plasma treatment generated a new peak at 289.0 eV due to O–C=O bond, whereas other polymeric films (i.e. PE, PP and PLA) had the same peak of XPS spectra but it has

the increase of percent peak area, as shown in Table 4.3. According to Table 4.4, the content of C1s decreases while the content of O1s increases and O/C ratio on the surface of plasma-treated films increased. These results suggest that oxygen was incorporated into the surface of polymer when treated by plasma. The introduction of oxygen-containing polar groups in polymeric surface may be the main reason for the hydrophilic improvement (Zhang and Fang, 2009). The increase of hydrophilic could be explained that some of C–C and C–H bond in polymeric surface may be broken by the DBD plasma which then created radical species on polymeric films. This species can combine with oxygen in air contributing to increase the amount of polar groups such as –OH, C=O, COOH and COO– on the plasma-treated surfaces (Sanchisa et al., 2008; Yang et al., 2009; Pandiyaraj et al., 2008). It has been generally believed that the oxygen was incorporated into the surface of all polymeric films by DBD plasma treatment and the hydrophilic groups were formed by interaction between the radical species on polymeric films and the oxygen in air (Choi et al., 1999).
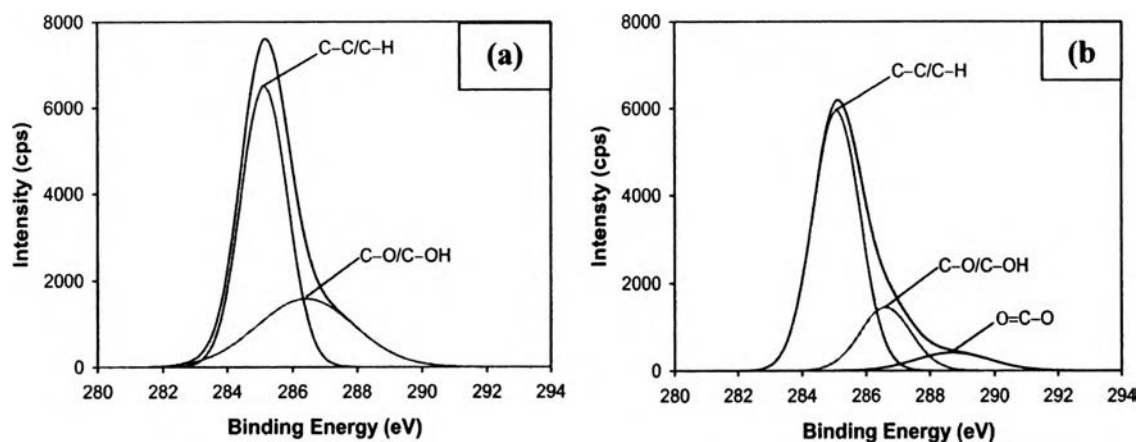

Figure 4.6 Deconvoluted XPS C1s core level spectra of PVC films; (a) before and (b) after plasma treated for 10 s.
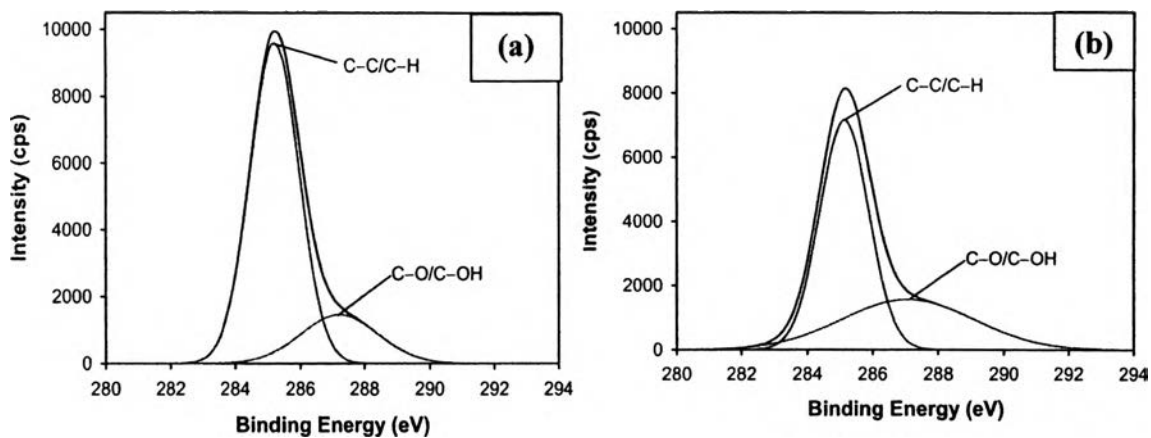
Figure 4.7 Deconvoluted XPS C1s core level spectra of PE films; (a) before, and (b) after plasma treated for 10 s.
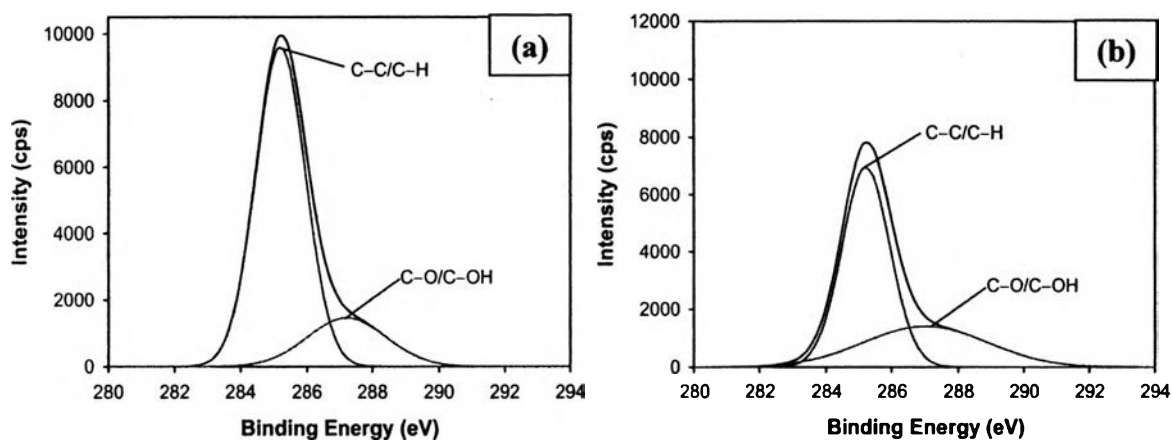

Figure 4.8 Deconvoluted XPS C1s core level spectra of PP films; (a) before, and (b) after plasma treated for 10 s.
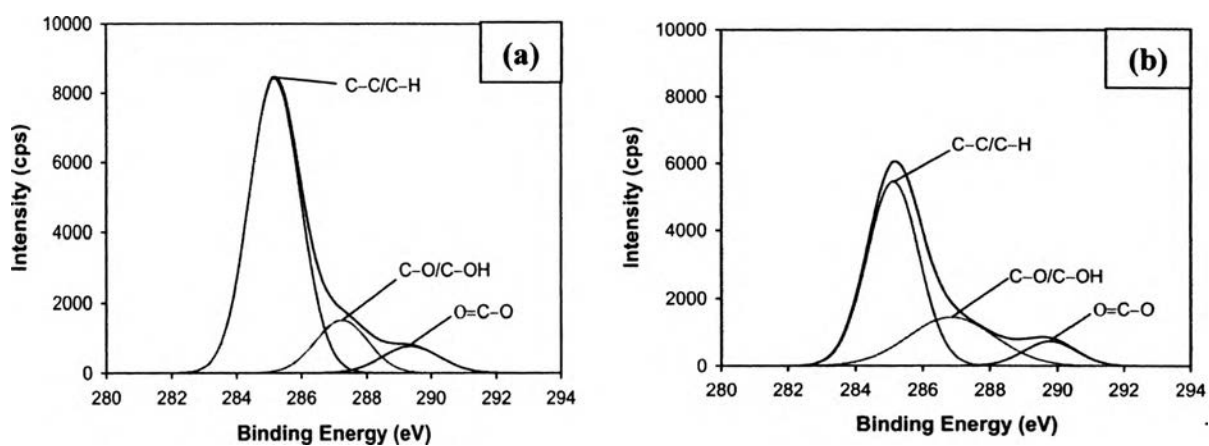
Figure 4.9 Deconvoluted XPS C1s core level spectra of PLA films; (a) before, and (b) after plasma treated for 10 s.

Table 4.3 Percent peak area of XPS C1s spectra of before and after DBD plasma in air of the PVC, PE, PE and PLA polymeric films for 10 s

Samples	Concentration of the different carbon-containing groups of polymeric films (%)		
	C–C (285.0 eV)	C–O (286.7 eV)	O=C–O (290.0 eV)
PVC Before treatment	86.32	13.68	0
After treatment	80.22	17.38	2.41
PE Before treatment	93.63	6.37	0
After treatment	89.12	10.88	0
PP Before treatment	93.31	6.69	0
After treatment	89.95	10.05	0
PLA Before treatment	85.43	9.87	4.70
After treatment	77.92	14.55	7.53

Table 4.4 Relative chemical composition and atomic ratios of four polymeric films determine by XPS

Samples	Chemical composition			Atomic ratios	
	C1s (%)	O1s (%)	N1s (%)	O/C	N/C
PVC					
Before treatment	69.34	28.36	2.30	0.41	0.033
After treatment	64.24	33.12	2.64	0.52	0.041
PE					
Before treatment	77.13	20.03	2.84	0.26	0.037
After treatment	69.78	27.42	2.81	0.39	0.040
PP					
Before treatment	79.19	18.55	2.26	0.23	0.029
After treatment	71.47	25.89	2.64	0.39	0.037
PLA					
Before treatment	62.12	36.20	1.69	0.58	0.027
After treatment	53.91	43.81	2.28	0.81	0.042

The samples were treated at power of 50 kV, frequency 325 Hz, gap distance 4 mm for 10 s.

4.2.4 Effect of DBD Plasma Treatment on Surface Morphology

The plasma treatment changes the physical properties on the surface of polymeric films were investigated by atomic force microscopy (AFM). The root mean square roughness (RMS) of before and after plasma treatment are shown in Table 4.5. The surface roughness value of all polymeric films was increased by DBD plasma treatment for 10 s. There are the occurrences of the prominent parts on the surface of all plasma-treated polymeric films (i.e. PVC, PE, PP and PLA) as shown in Figure 4.10, 4.11, 4.12 and 4.13, respectively. From these results, AFM images indicated that the surface roughness of all the plasma-treated films was increased due to the impact of plasma species leading to the removal of the top few monolayers on

the surface of polymeric films (Yang *et al.*, 2009). This phenomenon was earlier reported by Sanchis *et al.*, (2006) in that, it related with the weight loss and the etching process induced by the plasma treatment. This improves the surface energy and the adhesion between chitosan and polymeric films.
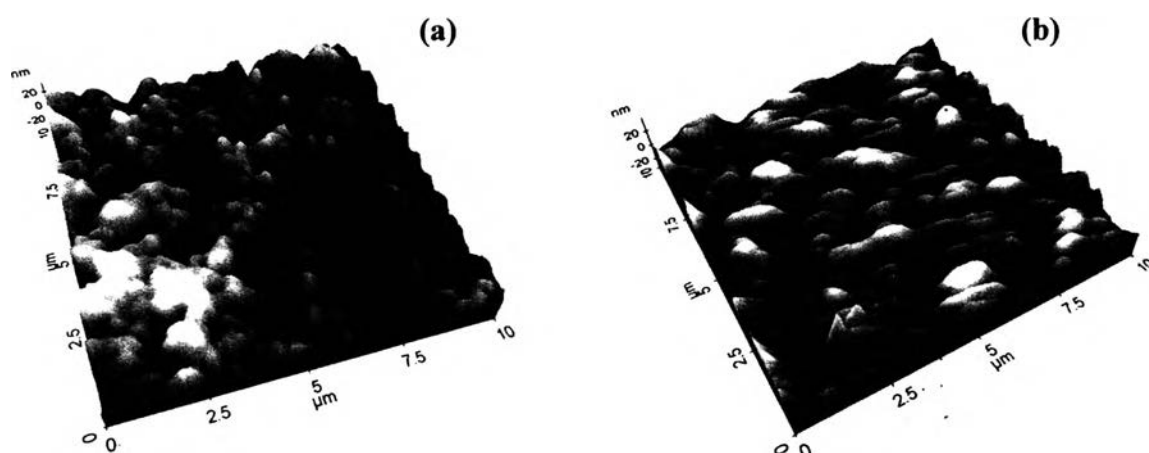

Figure 4.10 Three-dimensional AFM images of the PVC surface: (a) before plasma treatment; and (b) after plasma treatment for 10 s.
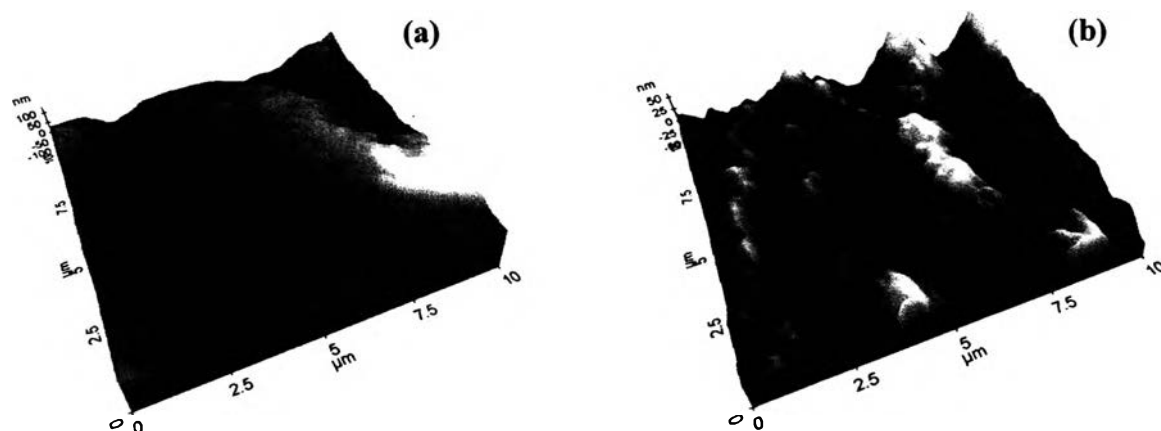

Figure 4.11 Three-dimensional AFM images of the PE surface: (a) before plasma treatment; and (b) after plasma treatment for 10 s.
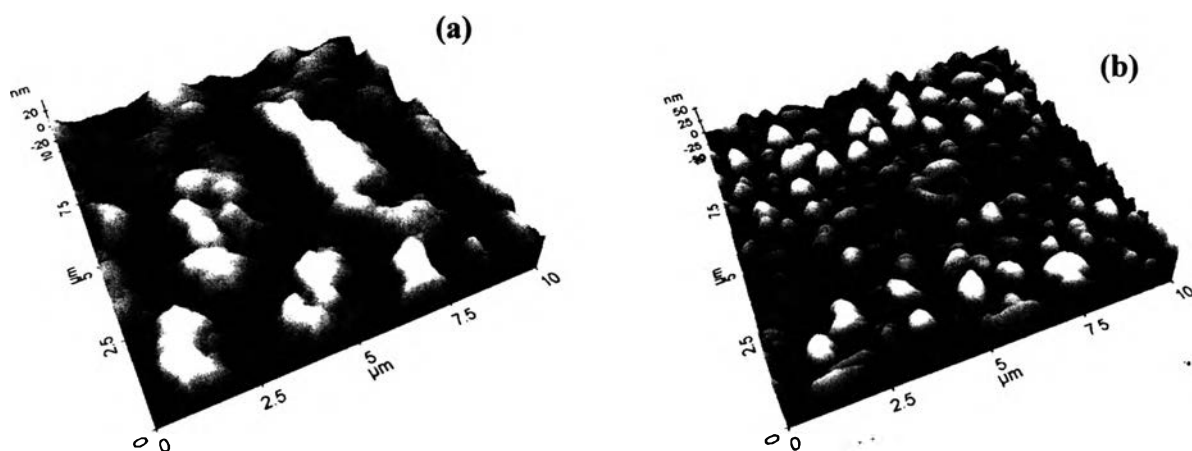
Figure 4.12 Three-dimensional AFM images of the PP surface: (a) before plasma treatment; and (b) after plasma treatment for 10 s.
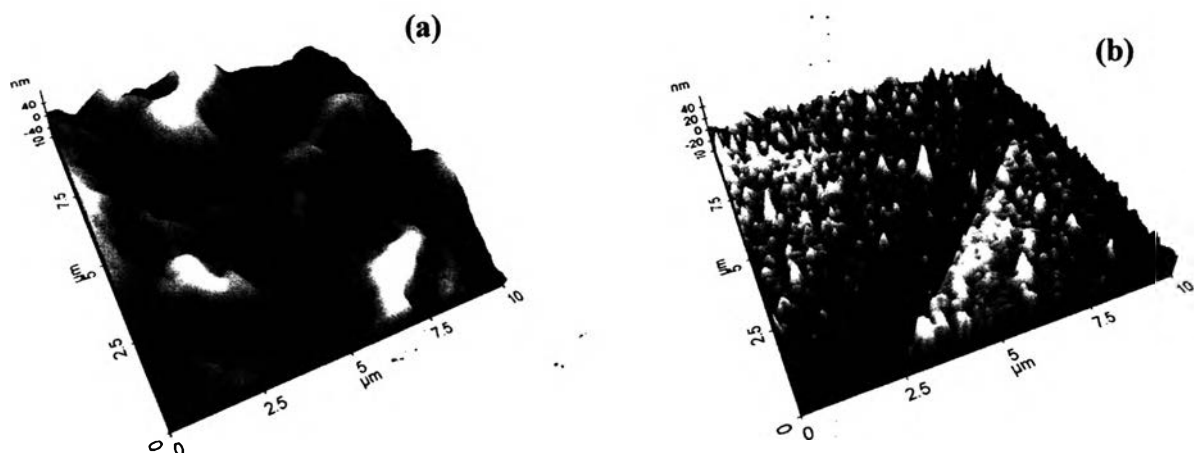

Figure 4.13 Three-dimensional AFM images of the PLA surface: (a) before plasma treatment; and (b) after plasma treatment for 10 s.

Table 4.5 The root mean square roughness (RMS) of before and after plasma treatment films

Type of polymeric films	RMS roughness (nm)	
	Before plasma treatment	After plasma treatment for 10 s
Polyvinyl chloride(PVC)	11.35 ± 0.86	16.43 ± 2.54
Polyethylene (PE)	29.35 ± 8.94	37.33 ± 9.03
Polypropylene (PP)	12.89 ± 2.57	17.45 ± 1.92
Polylactic acid (PLA)	10.33 ± 1.55	24.88 ± 4.97

4.2.5 Effect of The DBD Plasma Treatment on The Functional Group of The Plasma Treated Surfaces

Figure 4.14(a) shows the ATR-FTIR spectra of the PVC films before and after plasma treatment for 10 s. The original PVC film displays the band at 2930 cm^{-1} corresponds to –CH– stretching vibration. There are carbonyl groups in original PVC films at 1720 cm^{-1} corresponds to C=O stretching vibration, because of additive phthalate. The characteristic vibrational absorption of –C–Cl appeared in the spectrum of the PVC film ranging from 700 to 800 cm^{-1}. Comparing between before and after plasma treatment, there obviously appear new peak at 1646 cm^{-1} corresponds to COO– asymmetrical stretching vibration. In addition, the intensity of the peak related to C–Cl did not change, which suggests that the chlorine gas could not be removed by the DBD plasma for 10s. The ATR-FTIR spectra of the PE films and PP films of before and after plasma treatment for 10 s are shown in Figure 4.14(b) and 4.14(c), respectively. After plasma treatment for 10 s, the treated PE and PP films, there obviously appear the same new peaks at 1733 cm^{-1} corresponding to C=O stretching vibration. Ren et al., 2008 had also found similar group on surface of PE film after treated with DBD plasma in air. Figure 4.14(d) shows the ATR-FTIR spectra of the PLA films. The treated sample in time of 10 s, new absorption peak not obviously observe. These result suggests that oxygen functional groups such as the carbonyl group (C=O) and the carboxylate anions (COO-) were presented after plasma treatment. It might be postulated that the DBD plasma enhanced the

hydrophilicity of the polymeric films. An air plasma treatment can also lead to the production of radical species on the polymeric surface (Wilken *et al.*, 1999; Kuzuya et al, 1999). These radical species will take oxidation reaction with oxygen functional groups very easily (Chung *et al.*, 2004).
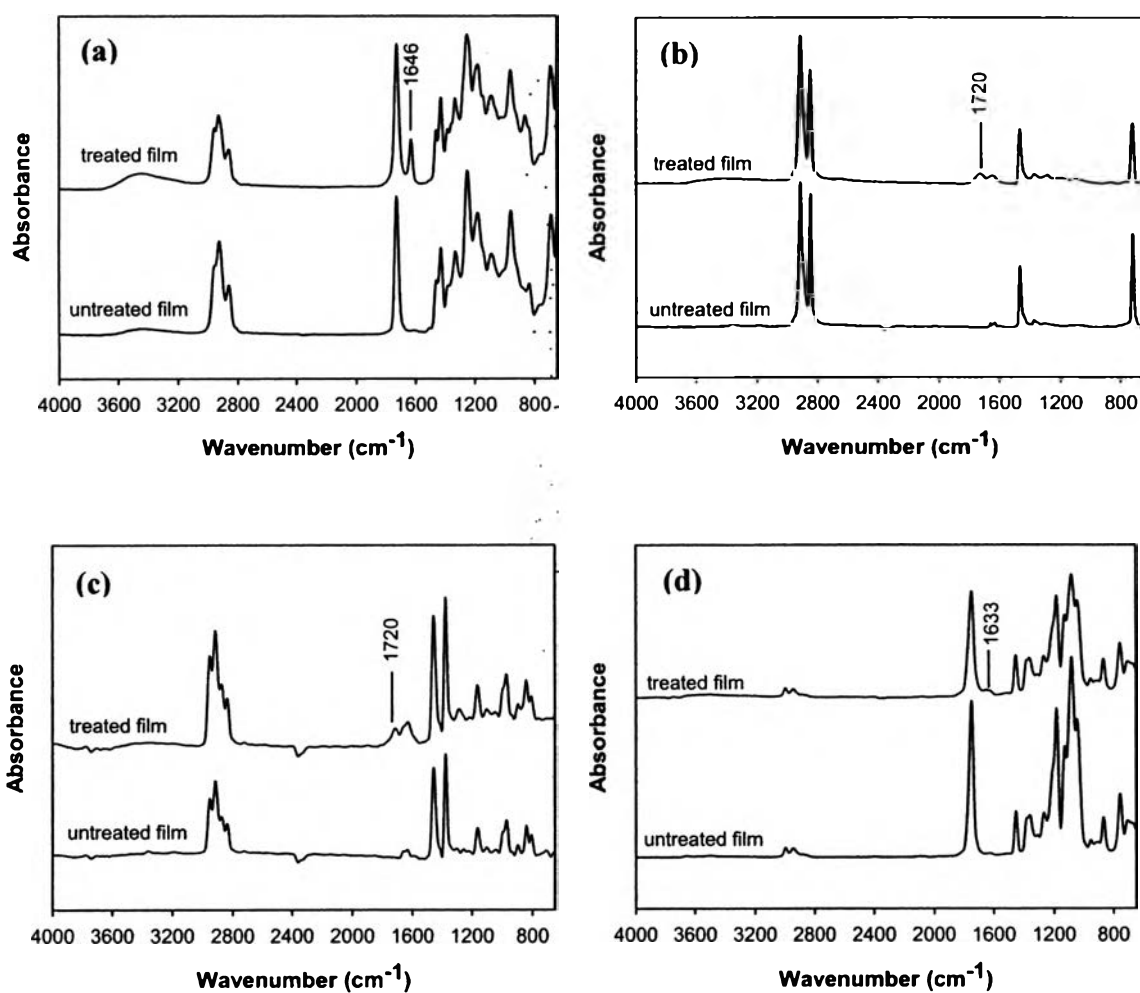

Figure 4.14 ATR-FTIR spectra of four polymeric films before and after plasma treatment for 10 s; (a) PVC films, (b) PE films, (c) PP films, and (d) PLA films.

4.3 Characterization of Chitosan-Coated Polymeric Films

4.3.1 Thermogravimetric Analysis

To confirm the presence of chitosan-coated polymeric films, TG-DTA was used. Figure 4.15(a) shows the TGA thermogram of PVC film, chitosan, PVC-2%CS. Thermal degradation of PVC showed in two steps, at 286°C was elimination of HCl leads to the formation of polyene sequences which then rearrange and decompose to aromatic and aliphatic hydrocarbons at 439°C. Chitosan showed two discrete weight losses at approximately 100 and 305 °C. These are caused by the loss of water and the degradation of chitosan chains, respectively (Thanpitcha *et al.*, 2006). For PVC film coated with 2% chitosan concentration (PVC-2%CS) exhibit three weight loss steps at 286°C, 305°C and 439°C. Figure 4.15 (b) shows the TGA thermogram of PE film, chitosan, PE-2%CS. Thermal degradation of PE showed at 460°C. For PE coated with 2% chitosan concentration (PE-2%CS) exhibit two weight loss steps at 305°C and 460°C. The TGA thermograms of PP film, chitosan, PP-2%CS are shown in Figure 4.15 (c). Thermal degradation of PP showed at 444°C. For PE coated with 2% chitosan concentration (PE-2%CS) exhibit two weight loss steps at 305°C and 444°C. Figure 4.15 (d) shows the TGA thermogram of PLA film, chitosan, PLA-2%CS. Thermal degradation of PLA showed at 353°C. For PLA coated with 2% chitosan concentration (PLA-2%CS) exhibit two weight loss steps at 305°C and 353°C. All of the polymeric films after coating with 2% chitosan concentration, exhibit weight loss at 305°C due to thermal degradation of chitosan. This result indicated that chitosan was incorporated onto surface of all treated films. In addition, thermal stability of all polymeric films did not change after coating with chitosan.
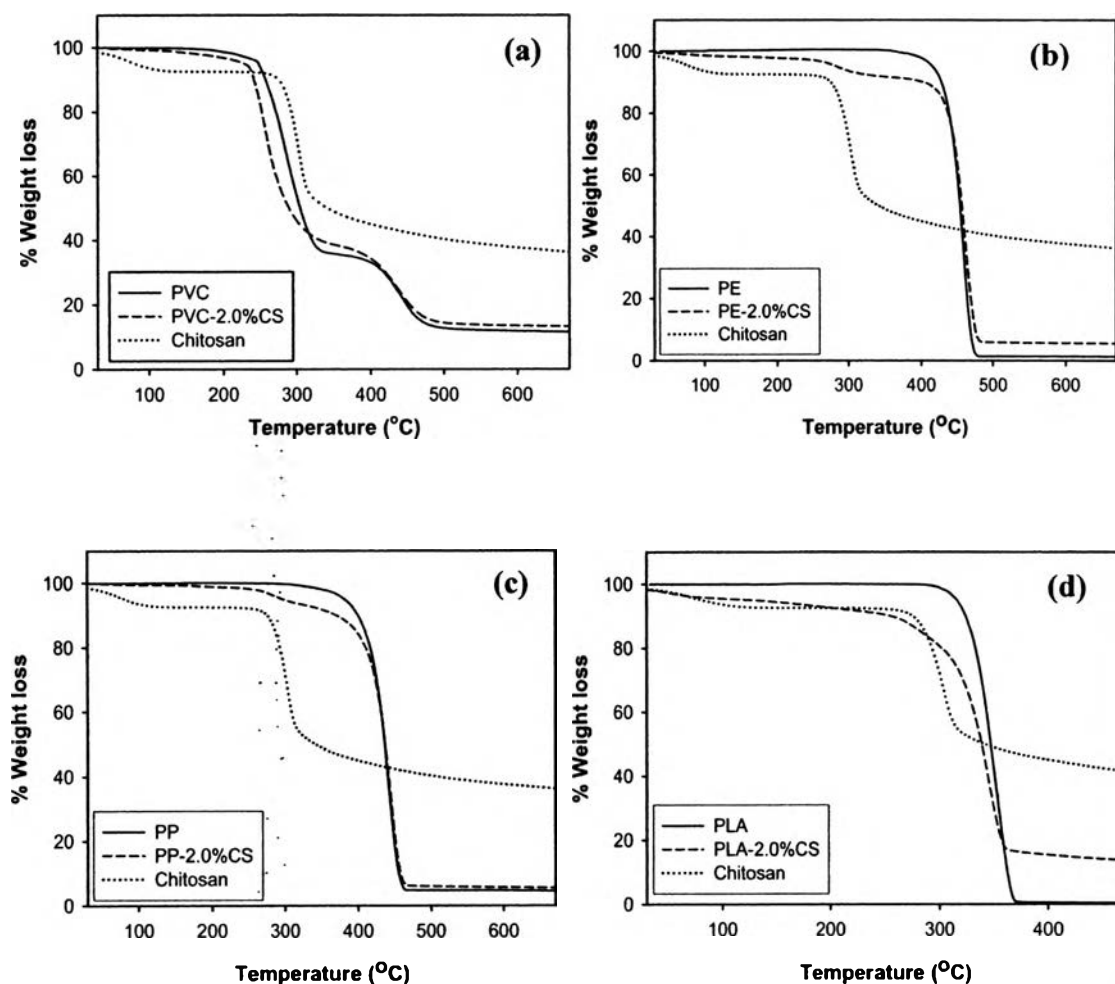
Figure 4.15 TGA thermogram of four polymeric films before and after coating with 2% chitosan concentration; (a) PVC films, (b) PE films, (c) PP films, (d) PLA films.

4.3.2 FTIR Spectra of Chitosan-Coated Polymeric Films in Different Concentration

The ATR-FTIR spectra for the treated PVC, PE, PP and PLA films and pure chitosan are shown in Figure 4.16 (A), 4.17 (A), 4.18 (A), 4.19 (A), respectively. For pure chitosan, the absorption peak at 3250 to 3460 cm^{-1} is due to overlapping of the OH and NH$_2$ stretches (Nunthanid *et al.*, 2004). Chitosan displayed characteristic absorption bands at 1655 and 1550 cm^{-1} which represent the amide I and amide II bands, respectively. The peak at 2922 cm^{-1} was due to the asymmetric bending of C–H group. Elsabee *et al.*, 2008 reported that the bactericidal effect should be proportional to the amount of chitosan on the surface therefore a

trial has been made to increase this amount of the adsorbed chitosan. The ATR-FTIR spectra for PVC, PE, PP and PLA films coated with chitosan in different concentration are shown in Figure 4.16 (B), 4.17 (B), 4.18 (B), and 4.19 (B), respectively. The ATR-FTIR spectra of all chitosan-coated polymeric films with chitosan in different concentration shows the new band characteristic for chitosan at 3450 cm^{-1} due to the stretching vibration of the NH$_2$. Obviously, with the increase of chitosan concentration, the relative strength of peak at 1655 cm^{-1} and 1550 cm^{-1} which represent the amide I and II absorption band of chitosan was increased. These indicated that all of chitosan concentrations were successfully coated on polymeric surfaces with DBD plasma technique. For PE and PP films at 0.75% to 2% chitosan concentration, there are obviously observed new peak at 1735 cm^{-1}. This points out that the covalent attachment of the chitosan into treated polymeric films could be occurred between a carbonyl group (C=O) of the treated polymeric films and amine group of chitosan.
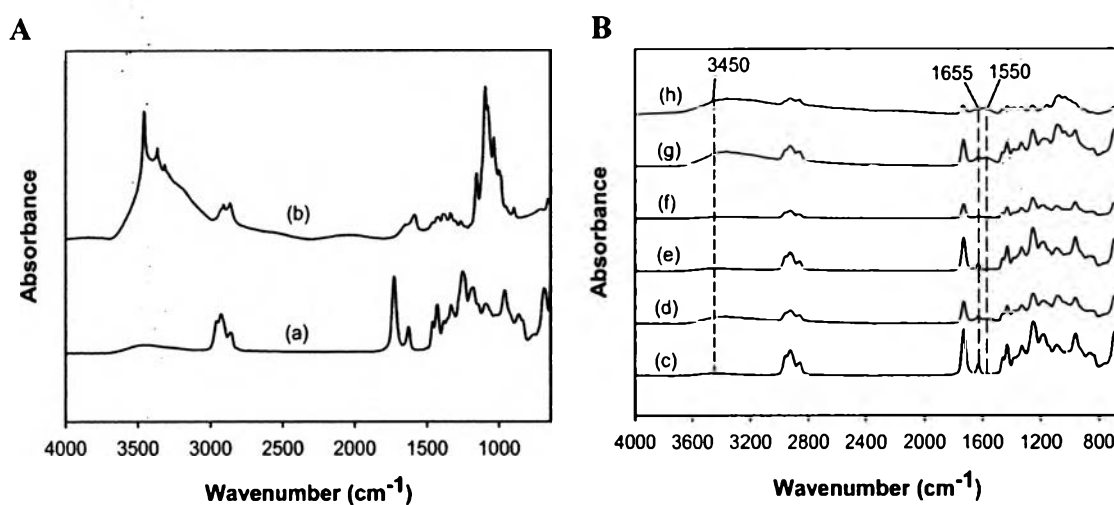

Figure 4.16 The ATR-FTIR spectra of treated PVC films, chitosan and chitosan-coated PVC films. (A) The treated PVC films (a) and chitosan (b); (B) chitosan-coated PVC films in different concentration of chitosan. (c) PVC-0.125%CS; (d) PVC-0.25%CS; (e) PVC-0.5%CS; (f) PVC-0.75%CS; (g) PVC-1.0%CS; (h) PVC-2.0%CS.
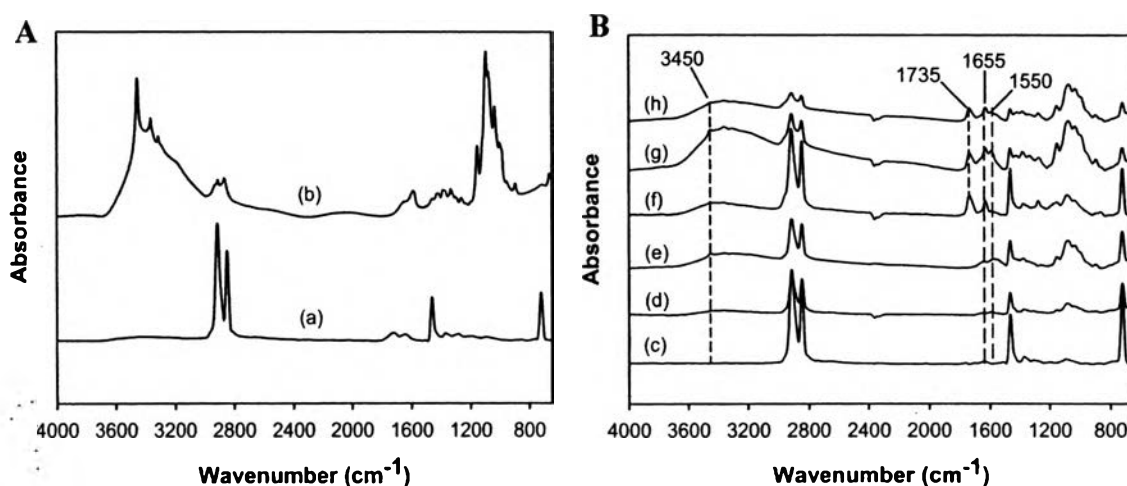
Figure 4.17 The ATR-FTIR spectra of treated PE films, chitosan and chitosan-coated PE films. (A) The treated PE films (a) and chitosan (b); (B) chitosan-coated PE films in different concentration of chitosan. (c) PE-0.125%CS; (d) PE-0.25%CS; (e) PE-0.5%CS; (f) PE-0.75%CS; (g) PE-1.0%CS; (h) PE-2.0%CS.
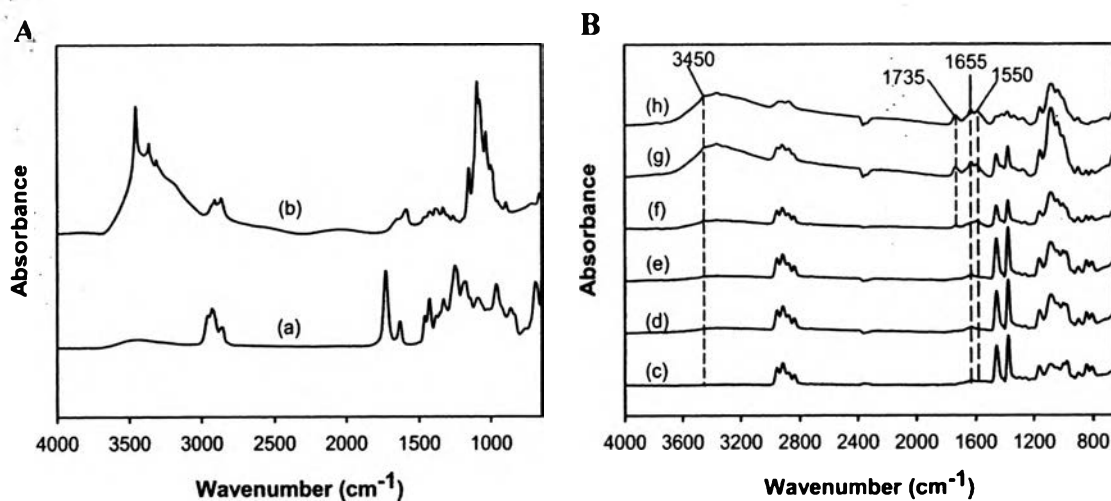

Figure 4.18 The ATR-FTIR spectra of treated PP films, chitosan and chitosan-coated PE films. (A) The treated PP films (a) and chitosan (b); (B) chitosan-coated PP films in different concentration of chitosan. (c) PP-0.125%CS; (d) PP-0.25%CS; (e) PP-0.5%CS; (f) PP-0.75%CS; (g) PP-1.0%CS; (h) PP-2.0%CS.
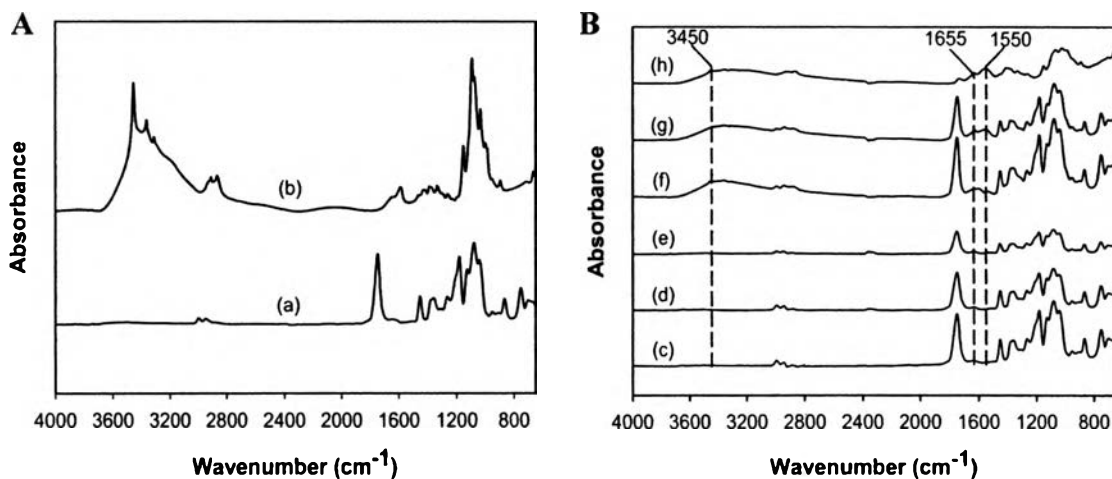
Figure 4.19 The ATR-FTIR spectra of treated PLA films, chitosan and chitosan-coated PLA films. (A) The treated PLA films (a) and chitosan (b); (B) chitosan-coated PLA films in different concentration of chitosan. (c) PLA-0.125%CS; (d) PLA-0.25%CS; (e) PLA-0.5%CS; (f) PLA-0.75%CS; (g) PLA-1.0%CS; (h) PLA-2.0%CS.

4.3.3 Effect of Number of Washing Cycle on Amount of Deposited Chitosan

Figure 4.20 shows the relation between the number of washing cycle and amount of deposited chitosan characterized by Kjeldahl method. The results of polymeric films coating with 2% chitosan solution shows that amount of the deposited chitosan on surface of all polymeric films decreased with increasing the number of washing cycle. The amounts of the deposited chitosan become constant after washing cycle for three times. This suggests that the excess amount of chitosan may be washed out on the surface during the washing cycle for one and two times. After washing cycle for three times shows the saturated amount of chitosan due to the formation of a strong chemical bond with treated films.
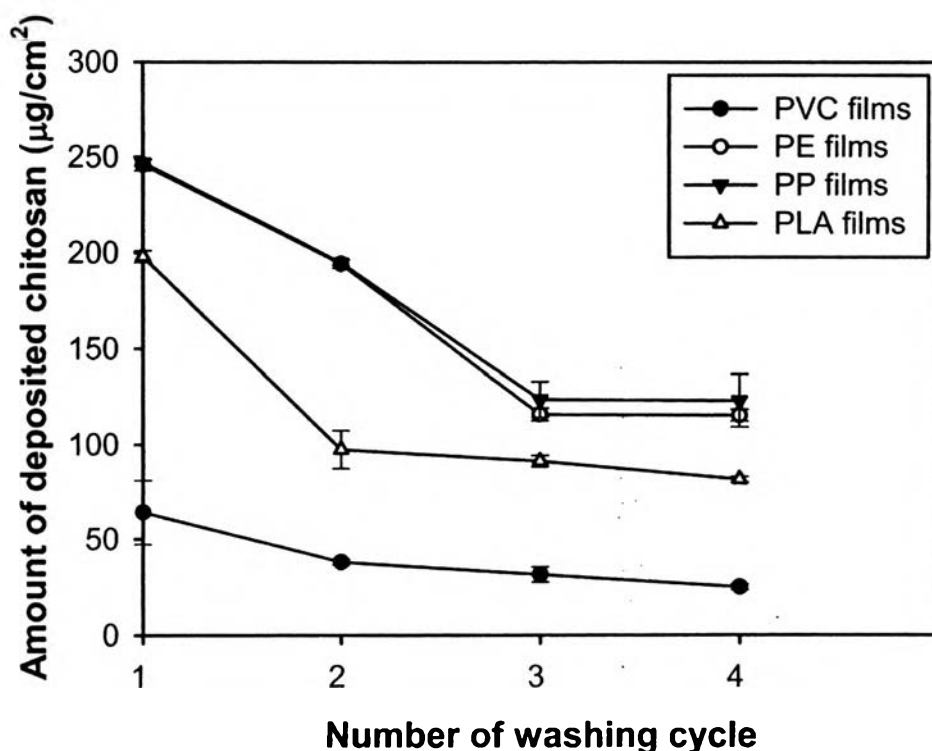
Figure 4.20 Effect of number of washing cycle on amount of chitosan deposited on four polymeric films.

4.3.4 Chitosan Content Determination

The amount of chitosan introduced on surface of polymeric films was determined by the Kjeldahl nitrogen analysis. Kjeldahl nitrogen analysis is the method for determining nitrogen in chitosan-coated polymeric films which were digested and then distilled into the trapping acid (HCl). The chitosan content was then calculated from back titration of trapping solution base on nitrogen content in chitosan. Figure 4.21 shows the relation between the concentrations of chitosan and the amount of chitosan deposited on untreated films and plasma-treated films of four polymeric films; (a) PVC films, (b) PE films, (c) PP films, and PLA films. For untreated films, chitosan was not deposited on the surface of all polymeric films. On the other hand, it was expected that after plasma treatment would increase the chitosan content onto the polymeric films. After plasma treatment, the amount of deposited chitosan on plasma-treated films increased with increasing concentration of chitosan from 0.1% to 2%. For 2% concentration of chitosan, the polypropylene

(PP) films were incorporated with the highest amount of chitosan, whereas the polyvinyl chloride (PVC) films were incorporated with the smallest amount of chitosan.
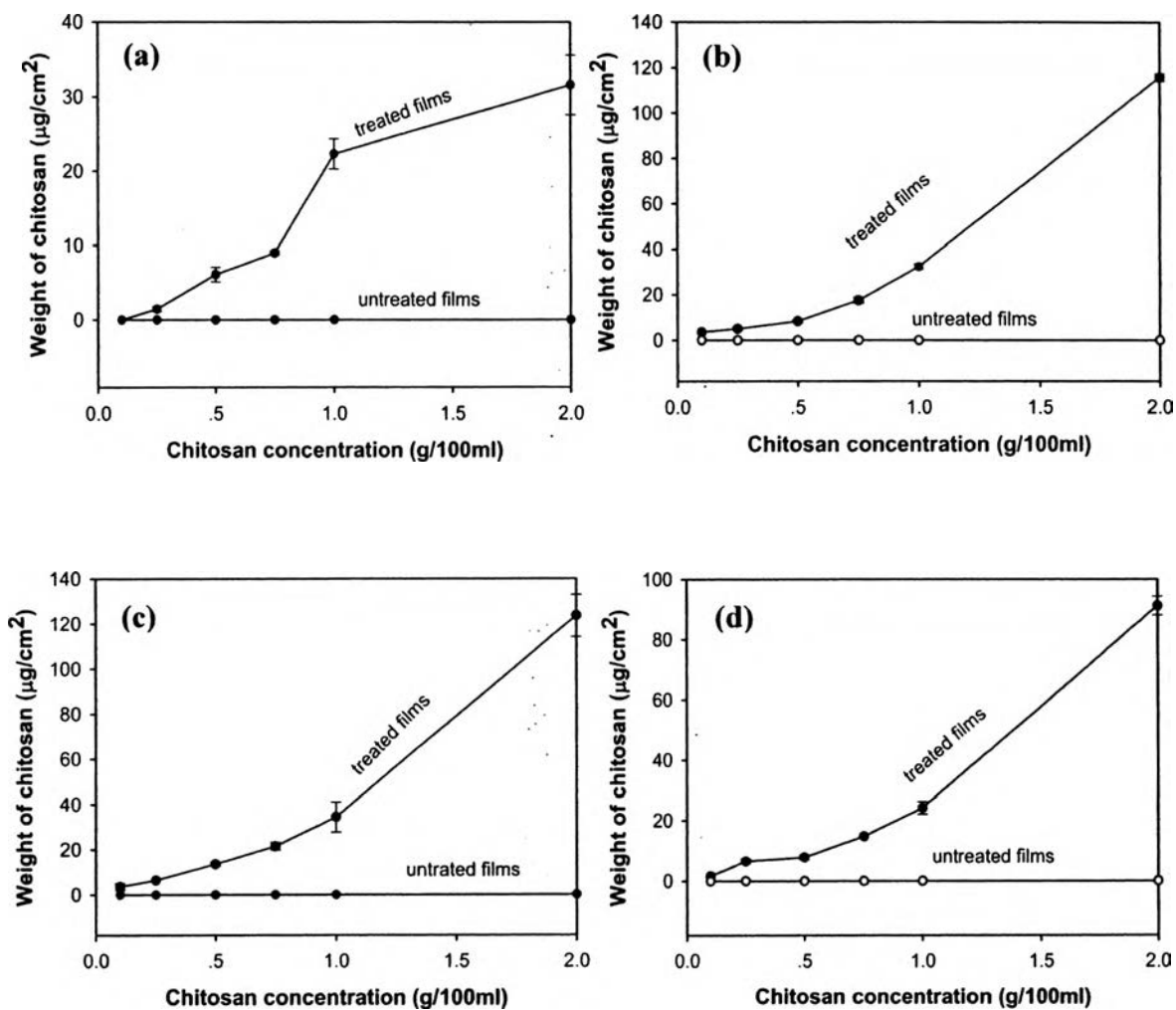

Figure 4.21 Relation between the concentrations of chitosan and the amount of chitosan deposited on untreated films and plasma-treated films of four polymeric films; (a) PVC films, (b) PE films, (c) PP films, and PLA films.

4.3.5 Staining of chitosan deposited on plasma-treated polymeric surfaces

The qualitative analysis of the deposited chitosan on polymeric films after plasma treated films could be investigated with amido black 10B. Amido black 10B is an amino acid dye used in biochemical research to stain the total amino group of chitosan. Owing to the positively-charged nature of chitosan, the anionic dye would selectively adsorb onto it. Figure 4.16 illustrates photographic of the neat polymeric films, the polymeric coated with 0.5 % chitosan concentration and the polymeric coated with 2% chitosan concentration, after they had been immersed in the aqueous solution of the dye for 12 h. It is evident that no specific interaction of all neat polymeric films with the dye was observed because there was no positively-charged to stain with the dye (Watthanaphanit et al., 2009). On the other hand, there was blue color appeared on the chitosan coated on all polymeric films. The distribution of the stained areas of 0.5% chitosan concentration coated on all polymeric films was not good. The stained areas distributed rather homogeneously throughout the polymeric coating with 2% chitosan concentration. This indicated that 2% chitosan concentration successfully incorporated onto all of polymeric films. These results clearly demonstrated that the air-plasma treatment improved the adhesion between chitosan and polymeric films.
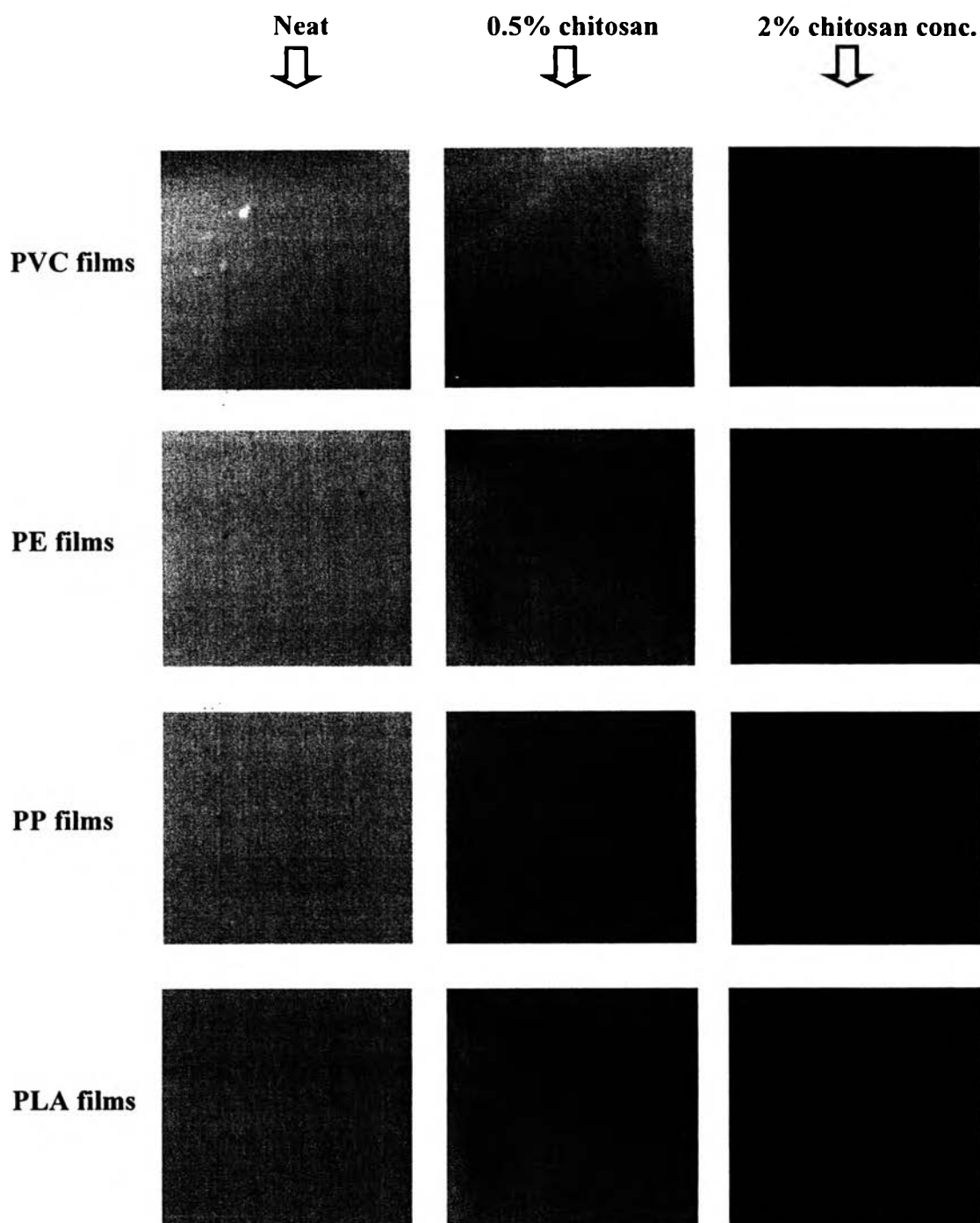
Figure 4.22 Photographic of the neat polymeric films, the polymeric coated with 0.5 % chitosan concentration and the polymeric coated with 2% chitosan concentration, after they had been immersed in the aqueous solution of the dye for 12 h.

4.4 Antimicrobial Activity of Chitosan-Coated Polymer Films

Development of a food packaging with antibacterial activity is important because packaging often provide favorable environments for colonization of microorganisms which may lead to degraded quality and shortened shelf life of food. The antibacterial properties of chitosan depend on its concentration, molecular weight, the degree of deacetylation and the type of bacteria (Chung *et al.*, 1998; No *et al.*, 2002). To prove the antibacterial activity, the chitosan-coated polymeric films with different concentrations (0.25%, 0.75%, and 2.0%) was tested against two commonly-studied microbes, i.e., Gram-positive *S. aureus* TISTR no.1466 and Gram-negative *E. coli* TISTR no. 780, by means of the colony count method. Number of colonies of neat polymeric films and chitosan-coated all polymeric films containing 0.25%, 0.75% and 2.0% of concentration of chitosan are shown in Figure 4.23. As can be seen, the antimicrobial activity increased with increasing concentration of chitosan on polymeric films. The bacterial reduction (BRR) values of the all polymeric films containing 0.25%, 0.75% and 2.0% concentration of chitosan against *S. aureus* and *E. Coli* are shown in Table 4.6. The result confirmed that all chitosan-coated polymeric films were responsible for the antibacterial activity and the activity is strong even if the concentration of the chitosan was low (i.e., 0.25% conc.). However, films with the highest chitosan concentration (i.e., 2.0%) showed the best reduction (BRR) values of both *S. aureus* and *E.Coli*. This suggests that a high percentage reduction of bacterial colony indicates a good antimicrobial activity of a sample. In addition, the proposed mechanism for chitosan antimicrobial relies on interaction between charges of chitosan and the microbial cell walls to block the nutrition supply and change the permeability of the cell walls, eventually causing death (Young and Kauss, 1983; Tokura *et al.*, 1997; Chan *et al*; 2001).
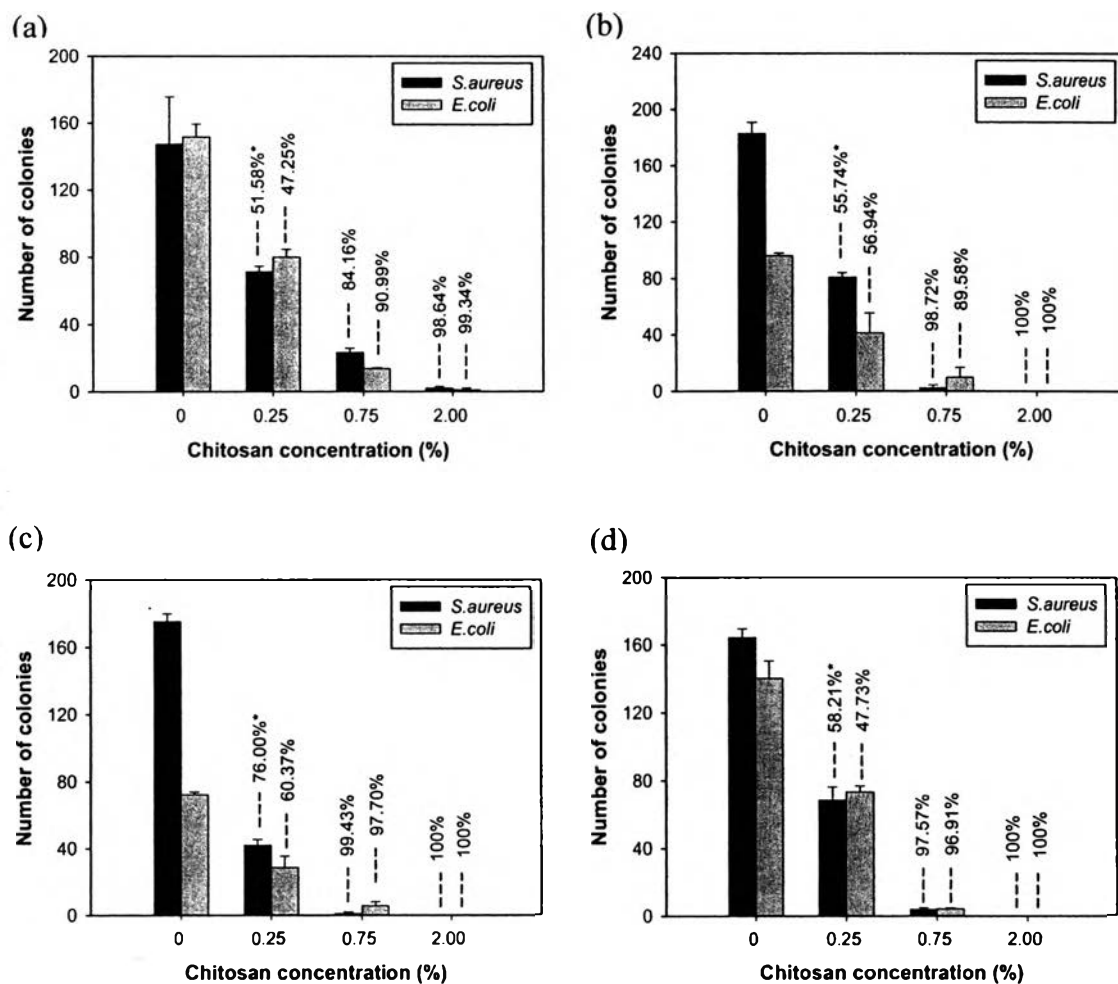
* The bacterial reduction (RRR%)

Figure 4.23 Number of colonies of neat polymeric films and chitosan-coated all polymeric films; (a) PVC films, (b) PE films, (c) PP films and (d) PLA films, containing 0.25% ,0.75% and 2.0% of concentration of chitosan and the corresponding bacterial reduction (BRR%) values against Gram-positive *Staphylococcus aureus* and Gramnegative *Escherichia coli*.

Table 4.6 Bacterial reduction (BRR%) of chitosan-coated polymeric films

Sample code	S. aureus	E.coli
PVC-0.25%CS	51.58	47.58
PVC-0.75%CS	84.16	90.99
PVC-2.00%CS	98.64	99.34
PE-0.25%CS	55.74	56.94
PE-0.75%CS	98.72	89.58
PE-2.0%CS	100	100
PP-0.25%CS	76.00	67.37
PP-0.75%CS	99.43	97.70
PP-2.00%CS	100	100
PLA-0.25%CS	58.21	47.73
PLA-0.75%CS	97.57	96.91
PLA-2.0%CS	100	100